



THÜNEN

Digitalization sponsored  
by Thünen-Institut

Not to be cited without prior reference to the authors.

International Council for the  
Exploration of the Sea

C.M. 1986/B:31 Sess.U  
Fish Capture Committee/  
Acoustic Methods

### ACOUSTIC IMAGING OF FISH

by

Tor Vidar Fosse and Halvor Hobæk

Department of Physics, University of Bergen, N-5000 Bergen

and

Magne Vestrheim, Chr. Michelsen Institute,

Dept. of Science and Technology, N-5036 Fantoft - Bergen, Norway

#### ABSTRACT

An acoustic imaging method has been used for the underwater imaging of fish bodies. The measurements were performed in a 4 cubic metres water tank and at a frequency of 512 kHz. The acoustic images of saithe (Pollachius virens) of lengths 0.33-0.36 m were obtained through measurements of the backscattered sound field from the fish at a distance of 1.0 m or 1.05 m with a simulated linear array of length 0.44 m or 0.7 m. A Fresnel approximation and a FFT (Fast Fourier Transform) routine were used in the signal processing needed for the image formation. The "one-dimensional" images for the length-dimension of the fish objects may provide such information as the extent of the fish in the head and tail directions. Further, the structure of the images provides information on the relative ability of different parts of the fish to reflect sound. Different characteristic image qualities can be distinguished towards the head and tail ends of the fish, respectively, and at the swimbladder.

## IMAGINE ACOUSTIQUE DE POISSONS

### Resumé

Des poissons ont été étudiés par une méthode d'imagerie acoustique. Les mesures ont été faites à 512 kHz dans un bac de 4 m<sup>3</sup>. Des images acoustiques de lieus noirs (*Pollachius virens*) de 0.33 à 0.36 m de long ont été obtenues en mesurant le champ retrodifusé par le poisson à des distances allant de 1.00 à 1.05 m, à l'aide de deux antennes linéaires différentes, de longueurs respectives 0.44 et 0.70 m. Le traitement du signal nécessaire à la formation des images, effectué par FFT (Fast Fourier Transform), se base sur l'approximation de Fresnel. Les images "unidimensionnelles", prises dans la direction de plus grande longueur de l'objet, indiquent la taille du poisson mesuré de la tête à la queue. En outre, l'étude de la structure des images montre comment le son est réfléchi par les différentes parties du poisson; Les régions de la tête, de la queue, et de la vessie natatoire, fournissent des images qui sont qualitativement différentes.

### INTRODUCTION

A traditional experimental way of studying the interaction of sound with a fish body is to measure the backscattered sound field in the acoustic far-field of the fish. Results from sonar far-field measurements of target strength, and the angular dependence of target strength with respect to the orientation of the fish in the sonar beam, are available in the literature. In addition, extensive modelling work to relate the complicated structure of the backscattered field to the anatomy of the fish is in progress (Foote 1985). Another experimental approach has been used in Sun *et al.* (1985), where a focused beam was used to measure the acoustic backscattering from local areas of the fish.

In the present paper, an acoustic imaging method is used to obtain an image of fish objects with good image resolution along the length of the fish. The image is in effect a reproduction of the sound field distribution over the object (the fish), and measures the local results of the interaction of the irradiating acoustic field with the fish.

This sound field distribution at the fish can be obtained from a remote sound field measurement through a data processing which performs a "backward propagation" on the measured sound field (Goodman 1968, Løvik 1977, Sutton 1979).

In order to investigate the potential of acoustic imaging techniques for applications in underwater viewing, an experimental underwater imaging system has been built at the Department of Physics, Univ. of Bergen. The system has so far been used primarily for imaging simple mechanical structures in order to study the functioning of the system and its basic imaging properties. On the initiative of Dr. Kenneth G. Foote at the Institute of Marine Research, Bergen, the use of the imaging system for acoustic imaging of fish was started. As is well known, fish bodies represent quite complicated structures in the interaction with sound waves, and the interpretation of the obtained acoustic images is more complicated than for simple mechanical objects.

The acoustic imaging system is described briefly here. Additional information concerning the present kind of imaging system can be found in, for instance, Sutton *et al.* (1974), Sutton (1979), Sutton *et al.* (1980), and Dalland and Vestrheim (1984). Some early results from the use of the method on the imaging of fish are presented. However, the work on interpreting the acoustic images obtained is far from complete.

## THEORY

A brief introduction to the theory used in the imaging technique is necessary in order to understand what is done. It is well known that a scattered sound field from an object can be transformed back from an observation plane to an object plane (e.g. Goodman 1968, Sutton 1979). A geometry for such a transformation is shown in Fig. 1, where the plane  $z=0$  is the object plane (and image plane), and the plane  $z=z_0$  is the observation plane.

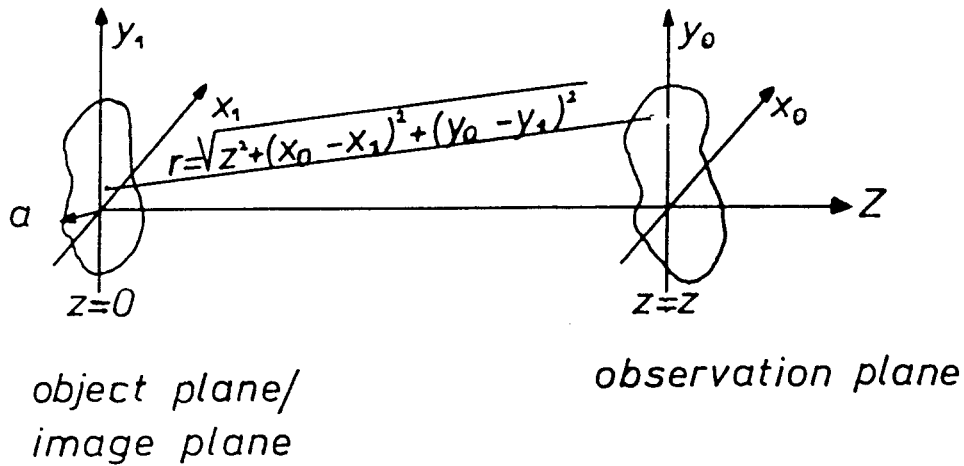


Fig. 1. Geometry for the acoustic imaging method.

The scattered sound field from the object is assumed to be sampled by measurements with a two-dimensional array in the observation plane. (However, in the present work only measurements with a simulated one-dimensional array along the  $x$ -axis have been made). In the theory the object is assumed to be ideally plane with a maximum dimension equal to  $a$ , and to be located in the object plane. The time dependence factor  $\exp(-j\omega t)$ , with  $j = \sqrt{-1}$ , has been neglected in the following equations.

The sound pressure at a point  $(x_0, y_0, z)$  in the observation plane can be written, as an approximation (Goodman 1968, Sutton 1979):

$$p(x_0, y_0, z) = \iint_{-\infty}^{\infty} h(x_0, y_0, z; x_1, y_1) p(x_1, y_1, 0) dx_1 dy_1, \quad (1)$$

where

$$h(x_0, y_0, z; x_1, y_1) = (1/j\lambda r) \exp(jkr), \quad (2)$$

and where

$p(x_0, y_0, z)$  : sound pressure at the observation plane

$p(x_1, y_1, 0)$  : sound pressure at the object plane

$h(x_0, y_0, z; x_1, y_1)$ : a transformation function which depends on

$\lambda$  = wavelength

$k = 2\pi/\lambda$  = wavenumber

$$r = \sqrt{z^2 + (x_0 - x_1)^2 + (y_0 - y_1)^2}$$

$z$  = distance from the object plane to the observation plane.

By using the Fresnel approximation (Goodman 1968) for  $z \gg a$ , Eq. (2) becomes::

$$h(x_0, y_0, z; x_1, y_1) \approx$$

$$[\exp(jkz)/j\lambda z] \exp\{(jk/2z)[(x_0 - x_1)^2 + (y_0 - y_1)^2]\}. \quad (3)$$

The approximation (3) can be used in Eq. (1) in order to write the integral in Eq. (1) in the form of a Fourier transform. The sound field in the object plane can accordingly be reconstructed from a sound field distribution in the observation plane through an inverse Fourier transform (Goodman 1968, Sutton 1979);

$$p(x_1, y_1, 0) = j\lambda z \exp(-jkz) \cdot \exp\left(\frac{-jk}{2z}(x_1^2 + y_1^2)\right).$$

$$\frac{1}{(2\pi)^2} \iint_{-\infty}^{\infty} p(x_0, y_0, z) \exp\left(-\frac{jk}{2z}(x_0^2 + y_0^2)\right) \exp\{j(k_x x_1 + k_y y_1)\} dk_x dk_y, \quad (4)$$

where

$$k_x = \frac{x_0}{z} k, \quad k_y = \frac{y_0}{z} k.$$

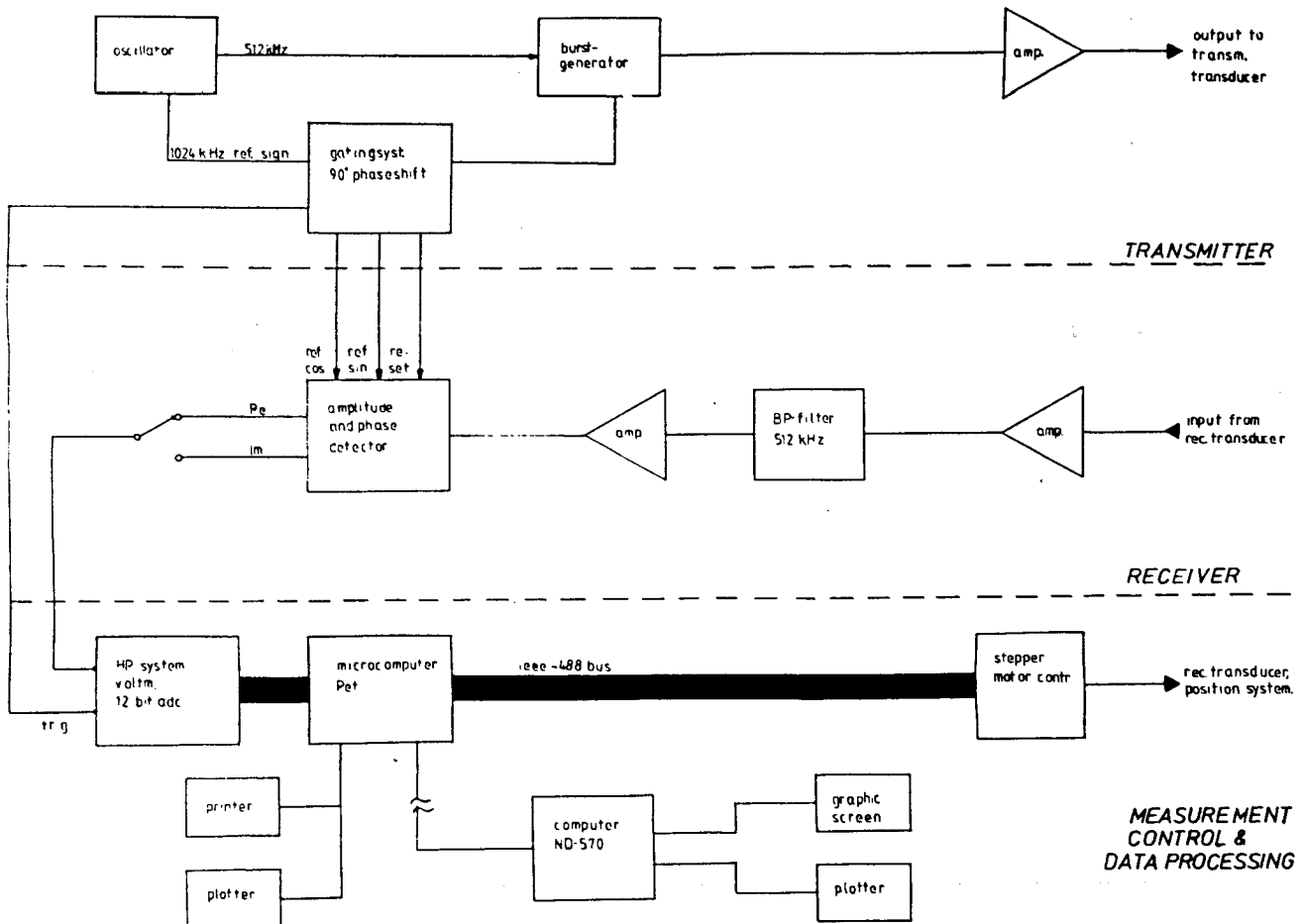
Here,  $p(x_1, y_1, 0)$  is now the reconstructed sound field distribution in the object plane, i.e. the image of the object. In the imaging technique used, the image of the object is found by performing the integration in Eq.(4), where  $p(x_0, y_0, z)$  is the observed pressure at the observation plane. The integration in Eq.(4) is performed through a Fast Fourier Transform routine. However, only a one-dimensional measurement of the scattered sound pressure has been made in the present work, and the integration in Eq.(4) is accordingly performed only in one dimension.

#### EXPERIMENT

The measurements were performed in a water tank of dimensions  $l \times w \times h = 4 \times 1 \times 1$  cubic metres. The instrumentation used in the acoustic imaging system is illustrated in Fig. 2a. A continuous wave (CW) signal of 512 kHz is formed into bursts and sent to the transducer which is used to irradiate the object. Acoustic CW bursts are used in order to reduce interfering effects of reflections from the water surface and the structures of the tank.

The scattered sound from the object is picked up by a hydrophone. The signal from the hydrophone is filtered, amplified and detected in the receiver electronics. In the receiver electronics the signal from the oscillator in Fig. 2a is also used as a reference signal. The input signal to the receiver,  $A \cdot \sin(\omega t + \varphi)$ , is mixed with the reference signal ( $\sim \sin \omega t$ ) and a  $90^\circ$  phase-shifted reference signal ( $\sim \cos \omega t$ ) and integrated over a number of periods of the received signal burst (see Fig. 2b). The results from the integrator are two constant "DC" output levels which are proportional to  $A \cdot \cos \varphi$  and  $A \cdot \sin \varphi$ , respectively, and which are sampled by a sampling voltmeter. Note that

a).

Holographic acoustic imaging system

b).

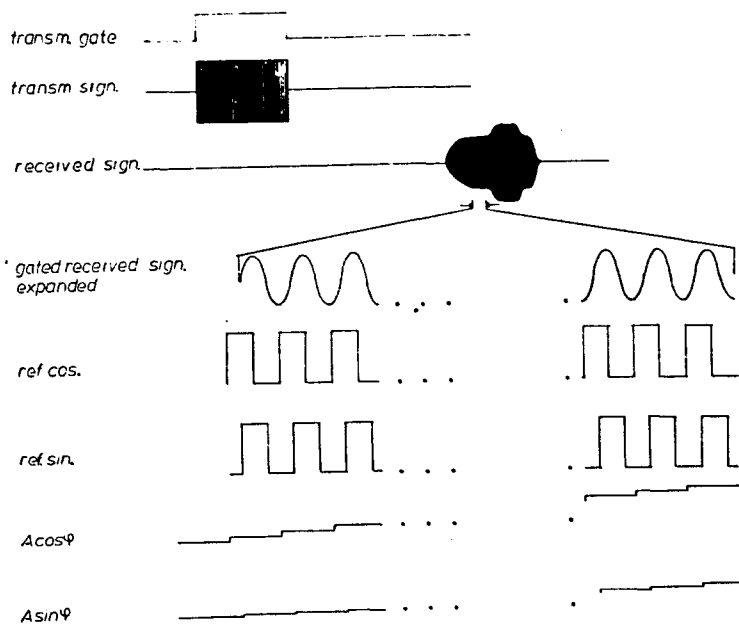


Fig. 2. The experimental acoustic imaging system.

a). Block diagram of the system, where the Transmitter, Receiver, and Measurement control & Data processing functions are indicated.

b). Pulse forms in the Transmitter and Receiver functions of the system.

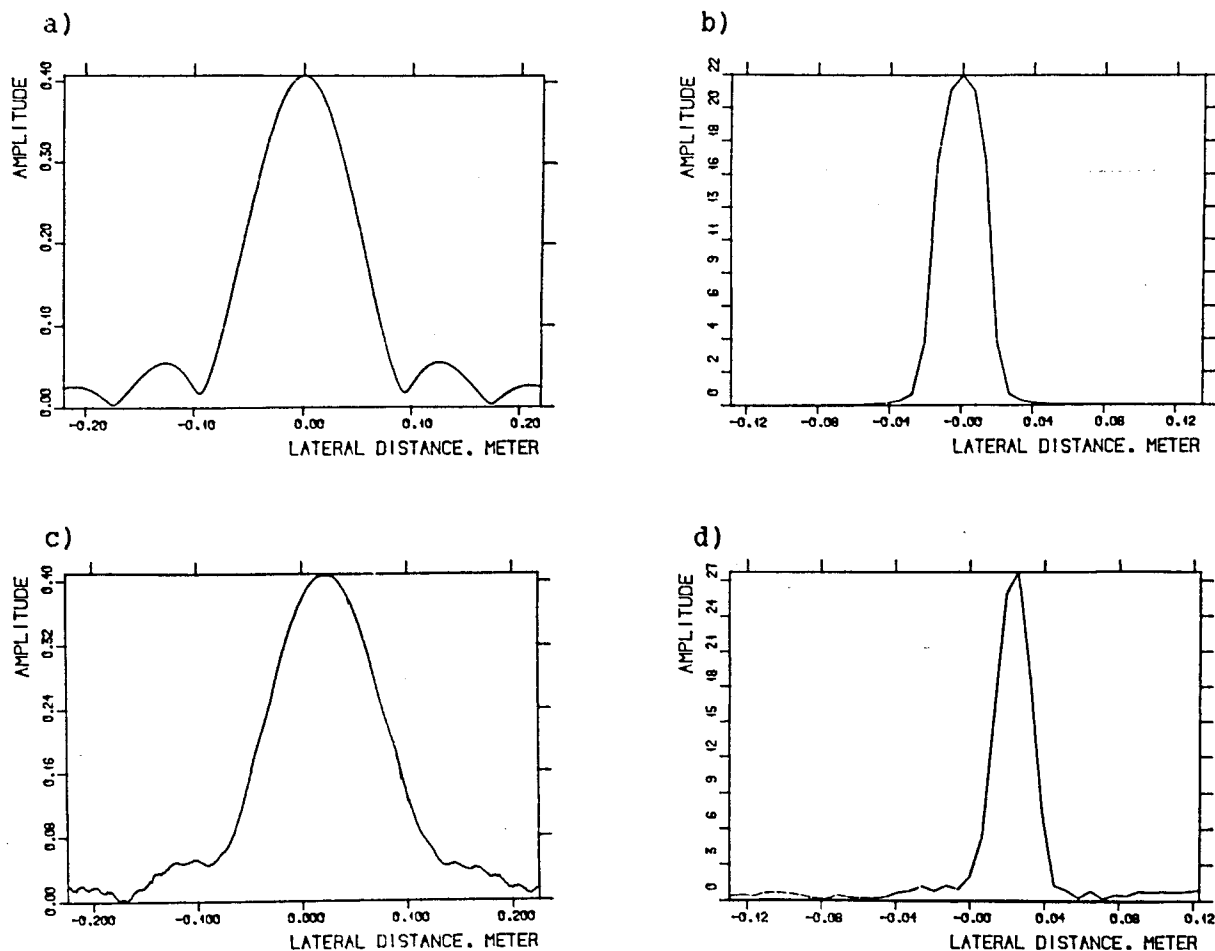


Fig. 3. Theoretical and experimental beam patterns and one-dimensional images for a circular piston source of radius 2.0 cm.

Distance:  $z = 1.0$  m. Array-length: 0.44 m.

a). Beam pattern. Theory. b) One-dimensional image. Theory. c). Beam pattern. Experiment. d). One-dimensional image. Experiment. The source used in c) and d) was also used for the measurements in Fig. 6.

different amplification settings have been used for different imaging measurements, in order to fully use the dynamic range of the receiver electronics.

A PET microcomputer controls the measurement sequences including mechanical scanning of the hydrophone, data sampling, data averaging, and data storage. The hydrophone is moved step by step across the sound field in order to simulate a receiver line array. Only one-dimensional measurements can be performed in the imaging system at present. The measured data can be printed and plotted by the microcomputer. In order to do the necessary processing for the "backward propagation" transformation, image formation and data presentation, the measured

data are sent from the microcomputer to a ND570 main computer.

The system has been used for imaging different mechanical objects which can be either active (the object radiates the sound itself) or passive (the object scatters the sound). As an example, the imaging of an acoustic circular piston type of source is shown in Fig. 3. Figs. 3a and 3b show theoretical results for the beam pattern and the one dimensional image, respectively, of a source of radius 2.0 cm, a distance of 1.0 m, and an array-length of 0.44 m. Figs. 3c and 3d show similar experimental results for the beam pattern and for the reconstructed one-dimensional image, respectively, of a source of radius 2.0 cm and for the same imaging geometry as assumed for a and b. The -3dB beamwidths for the theoretical and experimental beam patterns are seen to be  $4.3^\circ$  and  $5.0^\circ$ , respectively. In addition to a small relative displacement, the differences between the theoretical and experimental results are expected to be caused mainly by a nonuniform velocity distribution across the radiating face of the real source. The source with the beam pattern shown in Fig. 3c was also used for the measurements in Fig. 6.

The experimental arrangement for making the measurements on fish is shown in Fig. 4. The relative positions of the transmitting transducer, the object (the fish), and the receiving hydrophone are indicated. The hydrophone is scanned along a straight line normal to the length axis of the tank. The length of the scan defines the array-length. The midpoint of the simulated array defines the origin for the lateral distance in the observation plane. The origin for the lateral distance in the object plane and image plane is defined similarly by the intersection of the normal to the simulated array through the midpoint of the array and through the object/image plane.

A sketch of one of the arrangements used for mounting the (freshly killed) fish is shown in Fig. 5. A thin, transparent plastic bag was stretched across a metal frame. This allowed the fish to be slipped into the bag from the top side, thence reliably positioned. The frame was about 75 cm wide, allowing the fish to be moved back and forth inside the "plastic pocket" over nearly the whole width of the tank. In addition, the frame, which defines the "object plane", could be moved along the length of the tank to change the object range.

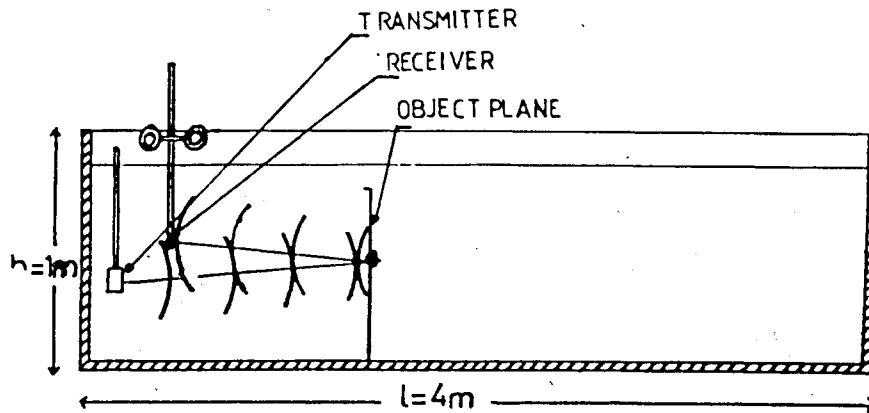


Fig. 4. The water tank seen from the side. The arrangement of the transmitter, the receiver and the object is indicated.

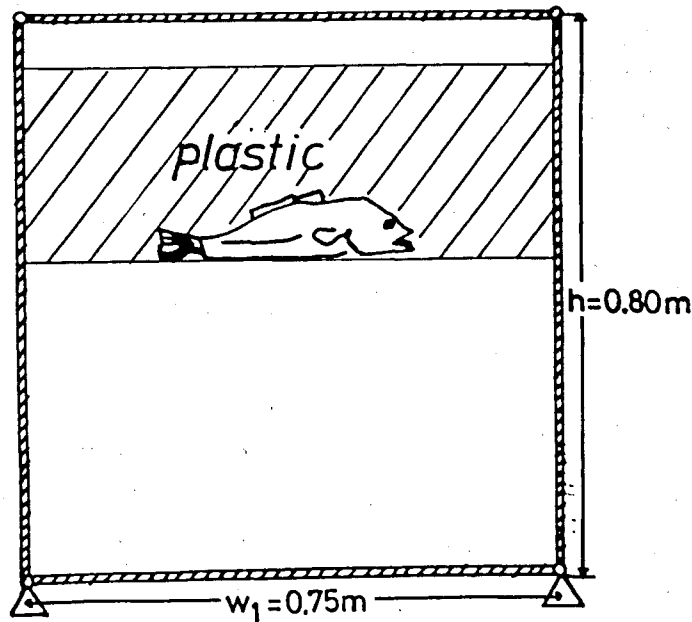


Fig. 5. The fish mounted in a plastic bag between the side bars of the frame.

One reason for using this mounting arrangement was to avoid the presence of air bubbles on the fish skin and in the gills and mouth regions. This mounting method was used for the imaging results in Fig. 6. However, it was experienced that the plastic bag alone provided a significant acoustic reflection, which could be strong enough to affect the images of the fish. Accordingly, another mounting method was used for some of the measurements, such as for the results shown in Fig. 7. In this latter method the fish was fastened to the top bar and the side bars of the frame in Fig. 5 with a thin line and small hooks. The acoustic reflection from this mounting arrangement (without the fish object) was tested and seen to be much smaller than the reflections from the empty bag in Fig. 5. However, the mounting procedure took

several minutes, while the fish was partly exposed to the air, and the checking of the mouth cavity and the gills for the presence of air bubbles was more difficult in this method.

A modification of the source was also made during the experiments. As can be seen from Figs. 3 and 6 the main lobe of the sound beam in fig. 3c covers only part of the fish. In order to obtain a more complete and uniform irradiation over the whole length of the fish objects, the sound source was altered by attaching a screen with a slit in front of the source. This provided a significantly broader acoustic beam (-3dB beamwidth of  $14.2^\circ$ ) over the fish. This modified source was used for the results given in Fig. 7, and the beam pattern over the fish object is shown in Fig. 7a.

## RESULTS

Some initial results on the acoustic imaging of fish are shown in Figs. 6 and 7. The measurements were taken at 256 equidistant points along the simulated receiving array. The gate window which was used for the integration in the receiver, covered 20 periods of the received signal.

In Figs. 6a-c results from the imaging of a saithe of length 0.345 meter is shown, and in Figs. 6d-f results from the imaging of another saithe of length 0.33 meter is given. For these measurements in Fig. 6 the source with the beam pattern given in Fig. 3c was used. The distance between the fish and the receiving hydrophone was 1.0 meter, and the hydrophone was scanned over an array-length of 0.44 meter.

In Fig. 6a the backscattered sound field from a saithe of length 0.345 meter is shown. This is the sound field received by the (simulated) receiving array, and which is used as an input to the processing needed for forming the image of the fish. (However, only the amplitude of the received sound field is shown in Fig. 6a). The sound field from the source was directed with its maximum intensity at the zero position on the lateral distance scale in the object plane.

Figs. 6b and 6c show two one-dimensional images of the same fish as used in Fig. 6a, and with the same direction of the irradiating sound beam. The two measurements were taken shortly after each other without changing details in the experimental arrangements. The purpose was to check on the repeatability of this kind of measurement.

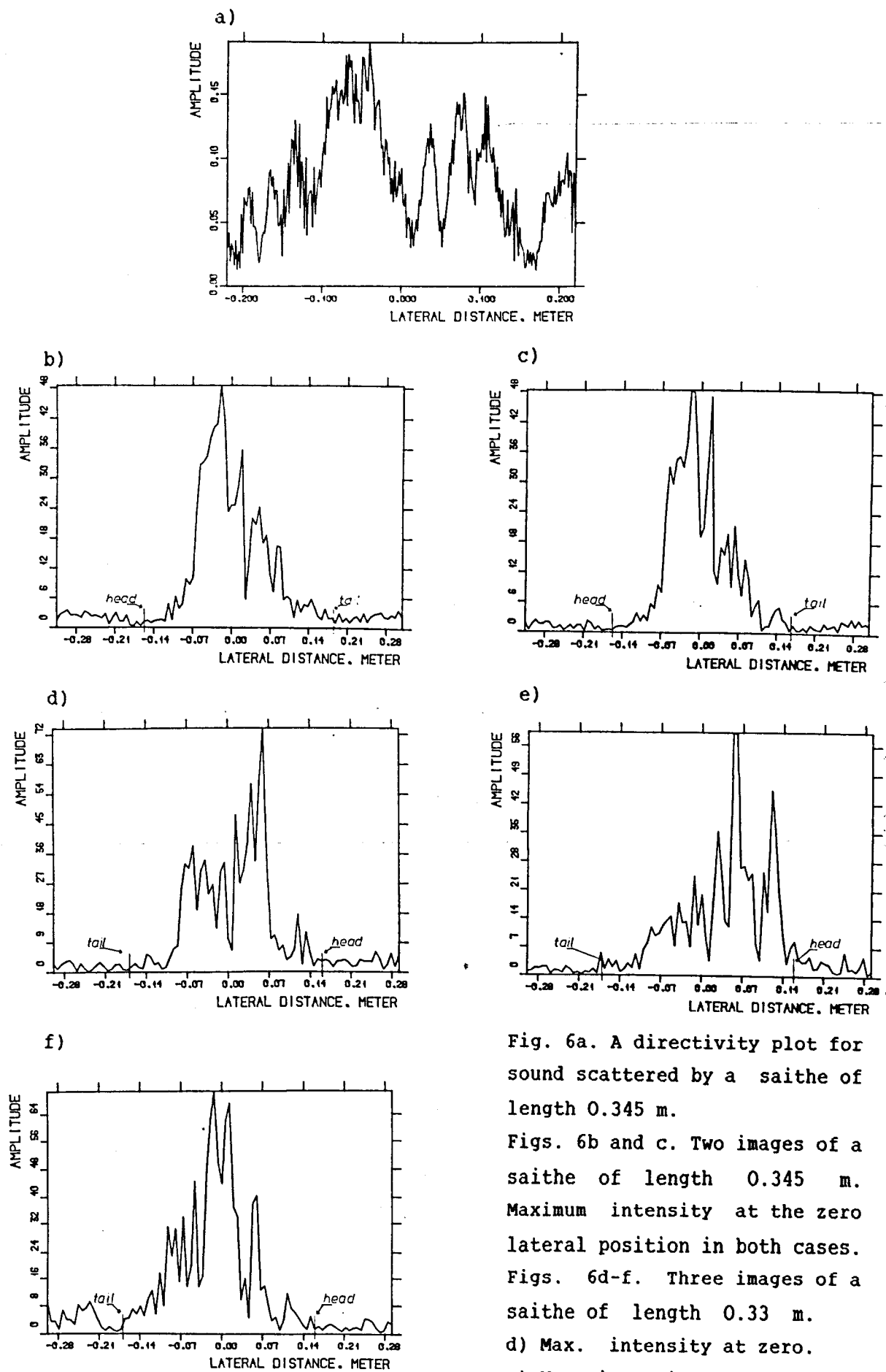


Fig. 6a. A directivity plot for sound scattered by a saithe of length 0.345 m.

Figs. 6b and c. Two images of a saithe of length 0.345 m. Maximum intensity at the zero lateral position in both cases. Figs. 6d-f. Three images of a saithe of length 0.33 m.

d) Max. intensity at zero.

e) Max. intensity at 0.11 m.

f) Max. intensity at -0.08 m.

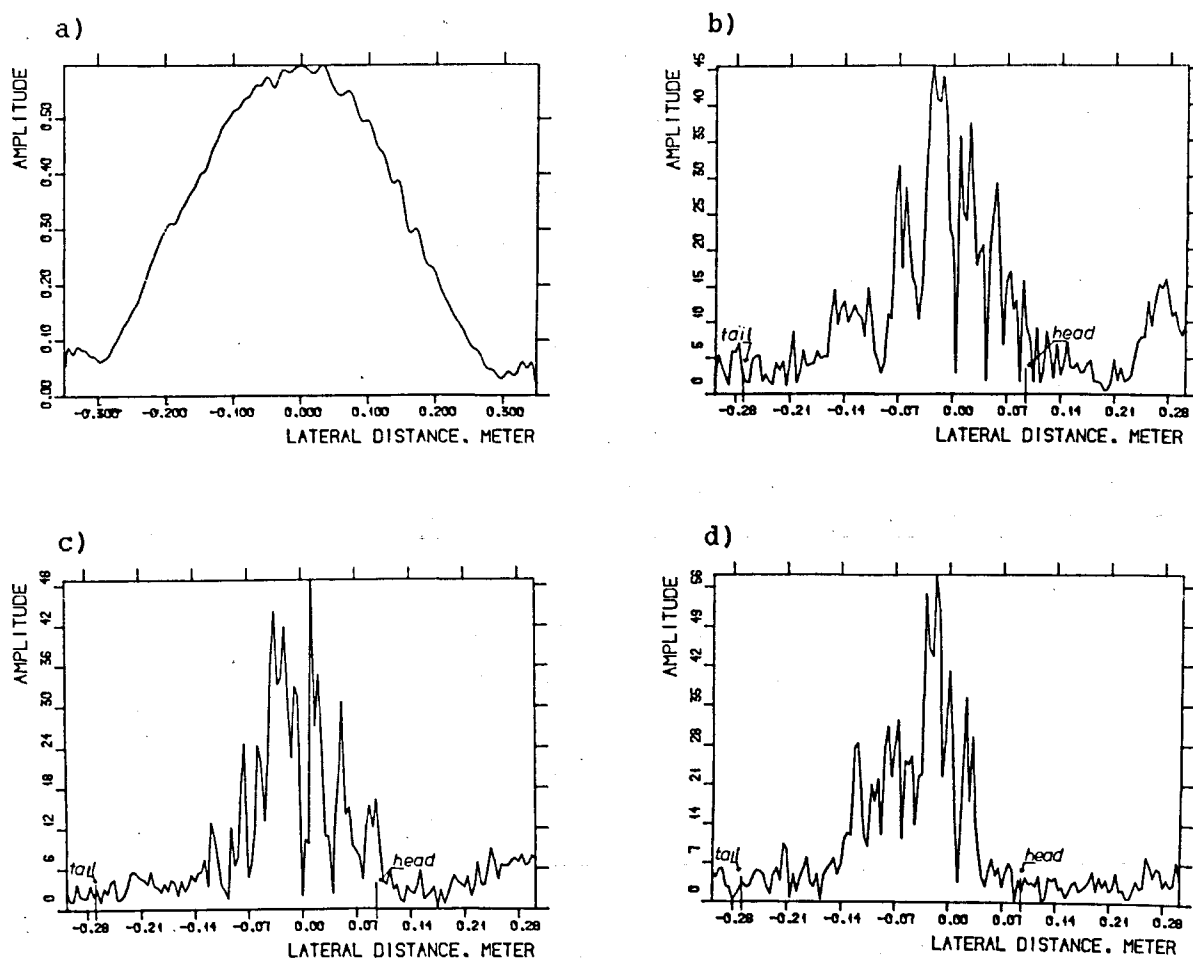


Fig. 7. Acoustic Imaging of a saithe of length 0.363 m.

- a) Beam pattern for the modified source used for irradiation.
- b) Acoustic image. Maximum intensity at -0.07 m.
- c) Acoustic image. Maximum intensity at 0.09 m.
- d) Acoustic image. Maximum intensity at -0.15 m.

Figs. 6d-f show similar images of the other saithe of length 0.33 meter. However, the directions for the irradiating sound beam were chosen with maximum sound intensity at lateral distances of 0.0 m, 0.11 m, and -0.08 m for Figs. d, e, and f, respectively.

For the results given in Fig. 7 the modified source with a broader beam pattern was used, and the fish was mounted by using a thin line and hooks, as described earlier. The distance between the fish and the receiving array was now 1.05 meter, and an array-length of 0.7 meter was used.

Fig. 7a shows the beam pattern of the modified source at a distance of 1.05 meter. Figs. 7b-c show images of a saithe of length 0.363 meter. The directions used for the sound beam were chosen with maximum intensity at lateral distances of -0.07 m, 0.09 m and -0.15 m, for Figs. b, c, and d, respectively.

## DISCUSSION

In discussing the results of the measurements it is important to be aware of several significant limitations in the experimental acoustic imaging method as it is implemented at present. Further development of the imaging system is expected to give considerable improvements in its imaging capabilities. Also, more experience in using the method and in processing and interpreting the results is needed in order to demonstrate the full power and potential of the method for the imaging of complicated objects such as fish.

The results in Figs. 6b and c show an example of the repeatability obtained when measuring a fish object. Even though the main structures in the image are reproduced, the differences in the images indicate that the repeatability may presently be insufficient for a more detailed study of the image structure.

The Fresnel approximation used in the processing needed for image formation, see Eqs. (3-4), may be insufficiently accurate for the array and object sizes and the observation distances used in the present experiment. The possible errors introduced can be checked by using a more accurate processing routine for the field transformation (Sutton 1979, Dalland and Vestrheim 1984).

The field is measured only along a finite line and not over a two-dimensional region of a plane. The resolution in the horizontal direction of the simulated line array will therefore be good, but the resolution in the vertical direction will be poor. In the vertical direction the resolution is determined by the beamwidth of the transmitting and receiving transducers. This resolution is so low that in practice the effect of the interaction of the sound with a full cross-sectional vertical "slice" of the fish will be seen in the images. The low resolution in the vertical direction also explains the shape of the image obtained for a circular piston source as shown in Figs. 3b and d.

As can be seen from Fig. 3c, the use of this source for the irradiation of the fish does not provide a uniform irradiation over the whole length of the fish. The -3dB beamwidth in Fig. 3c covers only a lateral length of 8.7 cm in the object plane, and the variation in field strength within the main lobe is large. This non-uniform irradiation explains some of the main features of the images. For example, if the main lobe is directed at the middle of the fish, as in Figs. 6b, c and d, the head and the tail of the fish cannot be discerned. In order to better resolve the head and tail part of the fish, the sound beam has been directed more towards the head in Fig. 6e, and more towards the tail in Fig. 6f.

To correct for some of the nonuniformity in irradiation, the modified source with the beam pattern shown in Fig. 7a, was used for the images in Figs. 7b-d. The -3dB beamwidth for this source represents a lateral distance of 26.2 cm in the object plane. This results in a considerable improvement, however, some variation in field strength still remains across the object.

The limited dynamic range in the receiving electronics is also seen from Figs. 6 and 7 to affect the information which can be obtained from the fish images. An increase in dynamic range of the order of 20 dB would improve this situation drastically.

Finally, another limitation in the imaging capabilities of the system is due to the use of "single-frequency bursts". Single-frequency-type holographic imaging systems are well known to give images affected by strong interference effects called "speckle". Such effects may explain some of the rapid variations in image amplitude as seen on the images. The interference effects can be reduced by techniques such as spatial filtering (which can be performed on the digital data in the computer, but which results in a lower resolution), and by performing the imaging over a frequency band.

Even with the limitations discussed above the initial results reported here are quite encouraging. The extent of the fish in the directions of the head and tail is indicated by the present images, and the fall-offs in the image amplitude towards the head and tail are different. The region of the fish where the swimbladder is located, is seen to give a large image strength. The relative image strengths obtained from the

different parts of the fish can also be compared roughly from these images.

#### CONCLUSIONS

Early results from the use of an acoustic imaging method on fish, already show that such a technique can be used to study several important parameters related to the size and structure of the fish. Work in progress will emphasize removing many of the limitations in the present imaging system which have been discussed here. The complete imaging operation can also be speeded-up towards close to real-time. With such improvements the acoustic method is expected to become a very powerful and versatile tool for performing studies and measurements on fish. Some of the parameters which may be studied through such acoustic imaging methods, are expected to be the size and orientation of single fish, the fish species, relative reflecting ability of different parts of the fish, existence and extent of the swimbladder, and counting and specification of fish individuals within schools of fish. In addition to the use of such information in more fundamental studies on fish, the data may also be of interest in the instrumentation and automatization of processes within the fishing industry, such as sorting and counting.

#### ACKNOWLEDGEMENTS

The use of the acoustic imaging method on imaging of fish was originally suggested by Kenneth Foote. His continued interest and comments have been of value throughout the work. Gunnar Alfheim has contributed to the construction of the experimental imaging system, and to the Figs. 2 and 4. Professor J. Naze Tjøtta is thanked for translating the abstract. The fish samples were obtained from the Aquarium of Bergen. The Norwegian Research Council for Science and the Humanities has provided some financial support to the initial buildup of the experiment.

## REFERENCES

Dalland, K., and Vestrheim, M. 1984. Simulation of imaging systems for underwater viewing. In Acoustical Imaging, Vol. 13, pp. 525-535. Edited by M. Kaveh, R.K. Mueller, and J.F. Greenleaf. Plenum Press, New York.

Foote, K. G. 1985. Rather-high-frequency sound scattering by swimbladdered fish. *J. Acoust. Soc. Am.*, 78(2): 688-700.

Goodman, J.W. 1968. *Introduction to Fourier Optics*. McGraw-Hill.

Lovik, A. 1977. Acoustic holography: A future method for underwater viewing? *Rapp. P.-v. Réun. Cons. int. Explor. Mer*, 170: 319-27.

Sun, Y. Nash, R., and Clay, C.S. 1985. Acoustic measurements of the anatomy of fish at 220 kHz. *J. Acoust. Soc. Am.*, 78(5): 1772-1776.

Sutton, J.L. 1979. Underwater acoustic imaging. *Proc. IEEE.*, Vol 67, No. 4, 554-566.

Sutton, J.L., Thorn, J.V., Booth, N.O., and Saltzer, B.A. 1980. Description of a Navy holographic underwater acoustic imaging system (AIS). In Acoustical Imaging, Vol. 8, pp. 219-234. Edited by A.F. Metherell. Plenum Press, New York.

Sutton, J.L, Thorn, J.V., and Prize, J.N. 1974. The effects of circuit parameters on image quality in a holographic acoustic imaging system. In Acoustical Holography, Vol. 5, pp. 573-590. Edited by P.S. Green. Plenum Press, New York.